2005

YBCO coated conductor using biaxially textured clad composite Ni-Mn/Ni-Cr substrate

D Q. Shi
University of Wollongong, dongqi@uow.edu.au

S X. Dou
University of Wollongong, shi@uow.edu.au

R. K. Ko
Korea Electrotechnology Research Institute, Korea

J K. Chung
Korea Electrotechnology Research Institute, Korea

H S. Kim
Korea Electrotechnology Research Institute, Korea

See next page for additional authors

YBCO coated conductor using biaxially textured clad composite Ni-Mn/Ni-Cr substrate

Abstract

A new biaxially textured composite tape of Ni–4.5% Mn/Ni–1.5% Cr was used as a substrate for a YBCO coated conductor through the RABiTS approach. Multi-layer CeO_2/YSZ/Y_2O_3 buffer layers and YBCO film were deposited on the substrate by pulsed laser deposition. The deposition conditions of the buffer layers and the YBCO were studied and compared. Good biaxial textures have been obtained for buffer layers on composite Ni–4.5% Mn/Ni–1.5% Cr substrates. Scanning electron microscopy on sample cross-sections was used to examine the interface and diffusion of oxygen. The uniform formation of an Ni–Mn–O layer between NiO and the Ni–4.5% Mn layer was observed, and the Ni–Mn–O layer restricted the further growth of NiO layer, which was thin and not continuous, within the coated conductor during YBCO deposition at higher temperature and higher oxygen pressure. The J_c of YBCO films on these metal substrates was 1.5×10^6 A cm^{-2} at 77 K, 0 T.

Keywords

YBCO, coated, conductor, using, biaxially, textured, clad, composite, substrate

Disciplines

Engineering | Physical Sciences and Mathematics

Publication Details

Shi, D, Dou, SX, Ko, R, Chung, J, Kim, H, Ha, H, Song, K & Park, C (2005), YBCO coated conductor using biaxially textured clad composite Ni-Mn/Ni-Cr substrate, Superconductor Science and Technology, 18, pp. 1405-1409.

Authors

D Q. Shi, S X. Dou, R. K. Ko, J K. Chung, H S. Kim, H S. Ha, K J. Song, and C. Park

INSTITUTE OF PHYSICS PUBLISHING
Supercond. Sci. Technol. 18 (2005) 1405–1409
SUPERCONDUCTOR SCIENCE AND TECHNOLOGY
doi:10.1088/0953-2048/18/10/028

YBCO coated conductor using biaxially textured clad composite Ni–Mn/Ni–Cr substrate

D Q Shi[1,4], S X Dou[1], R K Ko[2], J K Chung[2], H S Kim[2], H S Ha[2], K J Song[2] and C Park[3]

[1] Institute for Superconducting and Electronic Materials, University of Wollongong, Australia
[2] Korea Electrotechnology Research Institute, Changwon, Kyungnam, Korea
[3] School of Materials Science and Engineering, Seoul National University, Seoul, Korea

E-mail: dongqi@uow.edu.au

Received 16 June 2005, in final form 12 August 2005
Published 5 September 2005
Online at stacks.iop.org/SUST/18/1405

Abstract

A new biaxially textured composite tape of Ni–4.5% Mn/Ni–1.5% Cr was used as a substrate for a YBCO coated conductor through the RABiTS approach. Multi-layer CeO_2/YSZ/Y_2O_3 buffer layers and YBCO film were deposited on the substrate by pulsed laser deposition. The deposition conditions of the buffer layers and the YBCO were studied and compared. Good biaxial textures have been obtained for buffer layers on composite Ni–4.5% Mn/Ni–1.5% Cr substrates. Scanning electron microscopy on sample cross-sections was used to examine the interface and diffusion of oxygen. The uniform formation of an Ni–Mn–O layer between NiO and the Ni–4.5% Mn layer was observed, and the Ni–Mn–O layer restricted the further growth of NiO layer, which was thin and not continuous, within the coated conductor during YBCO deposition at higher temperature and higher oxygen pressure. The J_c of YBCO films on these metal substrates was 1.5×10^6 A cm^{-2} at 77 K, 0 T.

1. Introduction

A high temperature superconducting (HTS) $YBa_2Cu_3O_{7-\delta}$ (YBCO) coated conductor which consists of a superconducting layer and a buffer layer (which is multi-layer thin films) deposited on flexible metal tape is expected to satisfy the requirements of practical applications of high temperature superconductors in electrical power devices operating at liquid nitrogen temperature. Two main methods have been used to obtain biaxial texture of the superconducting layer, which is required for high current-carrying capability of the HTS coated conductor. One method [1, 2] uses ionized-beam-assisted deposition (IBAD) to make the first thin film layer deposited on the polycrystalline metal tape biaxially textured, which is followed by subsequent epitaxial deposition of additional buffer layers and superconducting layer. The other method, called rolling-assisted biaxially textured substrate (RABiTS), uses biaxially textured metal tape which is made by heat treatment under controlled atmosphere following mechanical deformation, and the texture of the metal tape is transferred to the buffer layer and then up to the superconducting layer through epitaxial deposition [3, 4]. It has been shown that nickel is well suited as a substrate material for the RABiTS approach because it forms a very strong cube texture after rolling and recrystallization. In addition, it is more resistant to oxidation than e.g. copper, and the small lattice mismatch with the oxides used for buffer layers allows epitaxial growth of buffer layers and YBCO film. Current densities exceeding 10^6 A cm^{-2} at 77 K self-field have been achieved in the YBCO coated conductors made on textured Ni metal tape [5, 6]. The nickel, however, has disadvantageous properties: (i) the ferromagnetism of the nickel leads to magnetization losses in ac field; (ii) its low tensile strength after heat-treatment limits the possibility of thin tapes, which are necessary to obtain a high engineering current density (i.e. the current in the HTS divided by the whole cross sectional area of the tape) [7].

One method of solving these problems is using Ni-alloy substrate instead of pure Ni [8]. The ferromagnetic Curie

[4] Author to whom any correspondence should be addressed.

temperature can be suppressed by alloying, which can help decrease the ac losses. The strength of the tapes is also expected to be enhanced by alloying due to solid solution hardening. Elements that can suppress the ferromagnetism of Ni within the solubility region are V, Cr, Si, Al, Ti and Mo. Compared with a pure Ni substrate, Ni with a small amount of alloying exhibits significantly reduced ac losses and increased mechanical strength. However, for alloy substrates, in particular, Ni alloy substrates containing Cr, subsequent epitaxial growth of the first oxide buffer layer is very difficult. The deposition of epitaxial oxides directly on the Cr-containing alloy results in the formation of non-cubic Cr_2O_3. One way to get around this problem is to deposit a thin layer of Ni or Ni–W on the Ni–Cr alloy before the deposition of the first buffer layer. Another method is the design of a RABiTS clad composite substrate. These clad composite substrates were originally developed in Japan by inserting a core metal rod into a Ni pipe or by sandwiching a core metal sheet between two Ag plates, which was followed by subsequently cold rolling and annealing as in the usual RABiTS process [9]. The core metal is usually stronger and/or has better magnetic properties in order to improve the performance without losing the biaxial texture of the original tape on the outer layer.

There are many reports on RABiTS-based coated conductors that used Ni alloy substrates. Until recently Ni–W tape has been the most commonly used for replacing pure Ni tape in the RABiTS process [10–13]. Some studies on coated conductors based on Ni–Cr tapes have been reported [14], and a clad composite Ni–Cr based tape has been used for the IBAD approach [9]. To my knowledge, there is no report about using Ni–Mn alloy substrate for a coated conductor. Adding manganese can control grain size and suppress abnormal grain growth during recrystallization and make grains more stable at high/low temperatures. Moreover, adding manganese can increase the ductility and high strain hardening capacity of the Ni–Mn tape [15]. In this study, clad composite Ni–4.5% Mn/Ni–1.5% Cr substrate was used as a substrate for a coated conductor through the RABiTS approach. The thermal expansion coefficients of the substrate (especially for Ni–1.5% Cr) can match both the buffer layers and the YBCO film within <10%. Buffer layers with the architecture of CeO_2/YSZ/Y_2O_3 were prepared by pulsed laser deposition (PLD). Deposition conditions, texture, microstructure and interfaces, and superconducting properties were studied.

2. Experimental details

PLD was used to deposit all oxide layers: CeO_2, Y_2O_3, YSZ, and YBCO. In the PLD system, stoichiometric Y_2O_3, YSZ, CeO_2 and YBCO ceramic targets 2 inches in diameter were mounted on a multiple target carrousel, which allowed all oxide depositions for the YBCO coated conductor specimens to be deposited in the same chamber *in situ*. The background pressure of the PLD chamber was less than 10^{-6} Torr. Biaxially textured clad composite nickel alloy (Ni–4.5% Mn/Ni–1.5% Cr) tape was obtained from a German supplier, which has a sandwich structure with a core layer of Ni–1.5% Cr and outside layers consisting of Ni–4.5% Mn. The total thickness of the substrate is about 0.11 mm, and the thickness of the Ni–Mn outer layer is greater than 10 μm. This tape has increased mechanical strength compared to pure Ni tape. The substrates used in this investigation had biaxial textures with in-plane and out-of-plane textures evaluated by the full width at half maximum (FWHM) of the ϕ-scan ($\Delta\phi$) and the ω-scan ($\Delta\omega$) of $\Delta\phi = 8°$–$10°$ and $\Delta\omega = 8°$–$9°$, respectively. 97% of the metal tape surface area was cube textured, as evaluated by pole figures.

The substrates, with a size of about 3×10 mm^2, were attached with silver paste to the target holder (also the heater), which was directly facing the target. The deposition temperature was measured by a thermocouple located in the heater block. The particulars of the deposition system were the following: fixed laser beam at an angle of 60° to the normal of the target; target–substrate distance 50 mm; target rotation 25 rpm. The deposition conditions were the following: laser repetition rate 5–20 Hz; the of the laser spot on the target 5×1 mm^2; pulsed laser energy density on the target 2–3 J cm^{-2}. Prior to deposition, substrates were heated from room temperature to the deposition temperature of Y_2O_3 in a 200 mTorr Ar/4% H_2 gas mixture, to prevent oxidation of the nickel substrate. Specimens were fabricated at different stages in the YBCO/CeO_2/YSZ/Y_2O_3/Ni architecture. This allowed for a study of the texture, smoothness, and microstructure of each of the deposited layers and the development of the stack.

The Y_2O_3 seed layer was deposited in 200 mTorr of Ar/4% H_2 for 1 min at a 5 Hz laser repetition rate. Then the laser repetition rate was increased to 10 Hz for 4 min. In a reducing atmosphere, the (00*l*) orientation of Y_2O_3 can be obtained over the wide deposition temperature range of 500–750 °C, which is basically due to the good lattice match between Y_2O_3 and Ni (lattice mismatch about 5.7%). After XRD ϕ-scan and ω-scan analyses, an optimal deposition temperature for the first step was chosen around 650 °C. The reducing atmosphere was removed by pumping to the base pressure of the system, which was $\sim 8 \times 10^{-6}$ Torr, and then the second part of the Y_2O_3 film was deposited. At this step, two deposition atmospheres were chosen and compared. One was 0.1 mTorr oxygen atmosphere, and the other was a vacuum below 8×10^{-6} Torr which was the base pressure of the deposition system used in this study. The biaxial textures of the Y_2O_3 films deposited under these two conditions are almost the same. From the point of view of preventing the undesirable formation of an NiO layer between the metal substrate and the Y_2O_3 layer, it should be advantageous to deposit Y_2O_3 in high vacuum at this stage. However, after our examination of the films, we found that the NiO layer and the Ni–Mn–O reaction and diffusion layers shown in the cross-section SEM image (figure 5) were not formed at this stage. The laser energy density on the target for Y_2O_3 deposition was maintained at about 2 J cm^{-2}. After the Y_2O_3 deposition, oxygen gas was then introduced into the chamber. After stabilizing the pressure at 1 mTorr the temperature was then increased from 650 to 780 °C, and the YSZ buffer layer was deposited for 20 min in the current oxygen atmosphere. For the YSZ deposition, the laser energy density on the target was increased to about 3 J cm^{-2} and the repetition rate to 20 Hz. Deposition times can be increased or decreased to change the thicknesses of the layers.

A cap layer of CeO_2 was deposited at the same laser energy density as for YSZ and at a repetition rate of 5 Hz

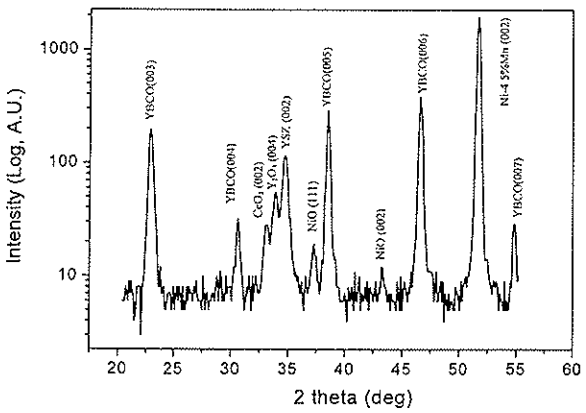

Figure 1. XRD θ–2θ scans for a typical YBCO/CeO_2/YSZ/Y_2O_3/Ni–4.5% Mn/Ni–1.5% Cr sample.

for 2 min. After deposition of the final buffer layer, the oxygen pressure was subsequently increased to 200 mTorr, and the superconducting YBCO layer was then deposited on the buffer layers. The YBCO film was deposited within a deposition temperature range of 770–790 °C in 200 mTorr oxygen pressure. The laser conditions were the following: energy of 150 mJ/pulse and repetition rate 10 Hz. Following deposition, the YBCO film was quickly cooled to 550 °C under the deposition pressure, and then kept for 20 min under an oxygen pressure of 500 Torr. It is not suggested that these are the optimal conditions for PLD of the various layers, but they are the ones used in this investigation.

The as-deposited films were analysed by a variety of characterizations. To study the crystalline alignment of the substrate, buffer layers and superconductor film, XRD θ–2θ scans, ω-scans and ϕ-scans were made to examine the textures of samples. The microstructure of the various films was investigated by scanning electron microscopy (SEM) with surface and cross-sectional views. A Digital Instruments atomic force microscope (AFM) was used to characterize the surface morphology and roughness of the buffer layers. Electrical property characterizations of the samples were made using a standard four-probe technique with a 1 μV cm^{-1} criterion to determine the critical current (I_c) as well as the transition temperature T_c. The thicknesses of the films were determined by etching the YBCO at an edge and measuring step height using a profilometer.

3. Results and discussion

To examine the epitaxial growth of the successive layers and determine the transfer of the biaxial texture of metal substrate to the films deposited on this, a series of XRD scans was taken. X-ray θ–2θ scans on the intermediate buffer layers of YBCO/CeO_2/YSZ/Y_2O_3/Ni–4.5% Mn/Ni–1.5% Cr architecture showed sharp (00l) peaks indicating excellent c-axis texture in buffer layers that was carried over to the superconducting YBCO layer (a typical figure is shown in figure 1). However, there were very small NiO (111) and (200) peaks that were likely to form during the YBCO deposition. ϕ-scans of the different oxide layers on the substrate indicate in-plane alignment of the various layers.

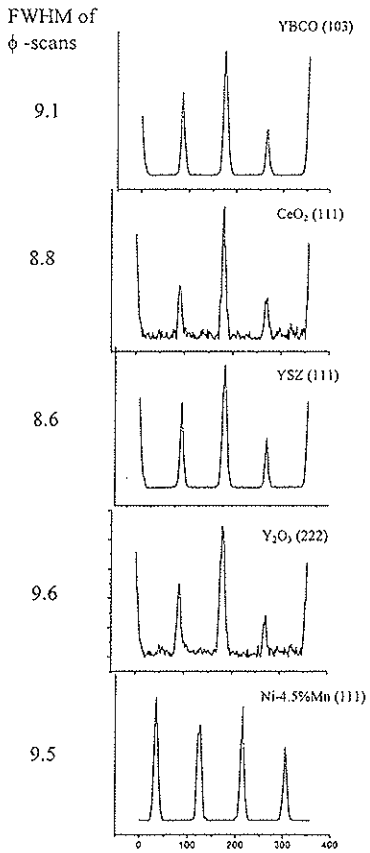

Figure 2. XRD ϕ-scans for the typical results of a YBCO/CeO_2/YSZ/Y_2O_3/Ni–4.5% Mn/Ni–1.5% Cr sample.

With a starting Ni–4.5% Mn with $\Delta\phi$ of 9.5°, the subsequent $\Delta\phi$ are for CeO_2 = 9.6°, YSZ = 8.6°, CeO_2 = 8.8° and YBCO = 9.1° (figure 2 shows these XRD ϕ-scans of a typical YBCO/CeO_2/YSZ/Y_2O_3/Ni–4.5% Mn/Ni–1.5% Cr sample). The role of YSZ was mainly as a barrier layer to prevent diffusion of oxygen and cation elements between YBCO and substrate. The relationship between superconducting properties of YBCO and the thickness of YSZ was analysed. YSZ layers were deposited with the thicknesses between 50 and 1000 nm at a deposition rate of about 35 nm min^{-1} while the thicknesses of other layers were kept constant. For this group of samples, the FWHM value of the XRD ϕ-scan for the (111) plane of YSZ did not change much with increasing YSZ film thickness, and the average value was about 8.2°, indicating that the in-plane alignment was not changed by increasing the thickness of the YSZ buffer layer. The J_c of the YBCO film was increased with increasing thickness of the YSZ, and the J_c remained about 1 MA cm^{-2} once the thickness was greater than 300 nm. Figure 3 shows the relationship between the FWHM of the ϕ-scan, the thickness of the YSZ film and the critical current density. Figure 4 shows the T_c and I_c plots of a typical sample. The I–V plot of the current measured in a typical specimen indicated that a 3.1 mm wide sample carried a critical current (I_c) of 10 A at liquid nitrogen temperature, which is equivalent to a J_c of 1.5 MA cm^{-2} at 77 K and self-field. The T_{c0} of the sample was 87.5 K.

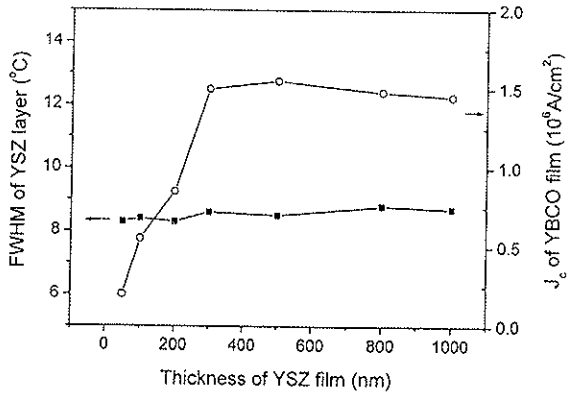

Figure 3. The relationship between the FWHM of the ϕ-scan, the thickness of the YSZ film and the critical current density of YBCO (the thicknesses of Y_2O_3, CeO_2 and YBCO were 60, 2.5, and 200 nm, respectively).

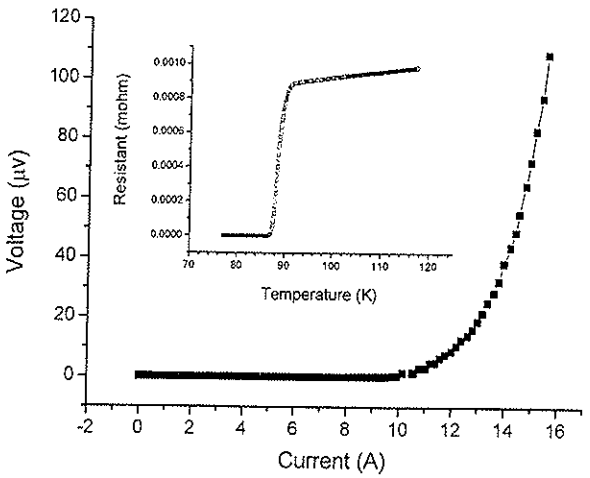

Figure 4. The I_c and T_c measurements of a typical YBCO/CeO_2/YSZ/Y_2O_3/Ni–4.5% Mn/Ni–1.5% Cr sample with the YBCO thickness 220 nm. The width of the sample was 3.1 mm.

Figure 5 is an SEM cross-sectional image of a YBCO/CeO_2/YSZ/Y_2O_3 sample. From the image, the thicknesses of Y_2O_3, YSZ, and YBCO were about 65, 290, and 130 nm, respectively. The thickness of the CeO_2 film was about 2.5 nm calculated by deposition rate and time. This layer cannot be seen clearly in figure 4 because it is too thin. The interfaces between Y_2O_3 and YSZ and also between YBCO and CeO_2 (YSZ in the image) were clean and smooth. The Y_2O_3, YSZ, and YBCO layers were dense from the SEM images.

The NiO layer identified by energy dispersive spectroscopy (EDS) during SEM of the cross-section, was present along the interface between the buffer and substrate. It was not uniform and not continuous. It should again be noted that NiO development within the sample occurred during the YBCO deposition process and not during the buffer layer deposition. The thickness of NiO depended on the deposition time of YBCO, e.g. the thickness of YBCO. In this image, the YBCO film is thin (about 130 nm) so the NiO layer is not continuous. The layer of material between the Ni–Mn layer and

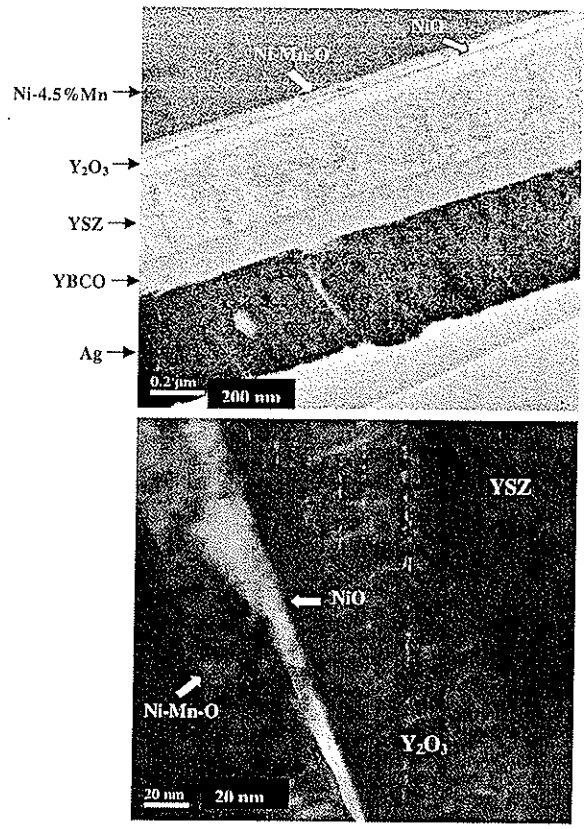

Figure 5. Cross-sectional SEM image of an YBCO/CeO_2/YSZ/Y_2O_3/Ni–4.5% Mn/Ni–1.5% Cr sample.

NiO was identified by SEM-EDS as consisting of Ni–Mn–O species. Because this Ni–Mn–O layer is also formed during the YBCO deposition, it does not damage the texture of the buffer layers. Unlike the NiO peaks in figure 1, the XRD θ–2θ scan cannot show evidence of the Ni–Mn–O layer, since there may be overlap with other peaks. The reason that the Ni–Mn–O layer was thicker than the NiO layer is that elemental Mn is more easily oxidized than Ni for a given amount of O_2. It is supposed that the formation of Ni–Mn–O between Y_2O_3 and the Ni–Mn/Ni–Cr substrate restricted the further growth of NiO within the coated conductor during YBCO deposition at higher temperatures and higher oxygen pressure. Although currently being investigated, the mechanisms responsible for the development of the Ni–Mn–O layer within the substrates are not fully understood. The EDS-SEM analysis cannot give accurate quantitative measure of the elements present, and further study is under way to identify the Ni–Mn–O phase.

An AFM image of the YBCO on top of the sample is given in figure 6. The outgrowths, or particulates on the surface, are evident here. The AFM scan on this specimen indicates that the R_{MS} roughness over a 20 μm × 20 μm area was about 57.4 nm including the outgrowths and was 26.7 nm over the same area if outgrowths are excluded. This can be compared to the roughness of the CeO_2 layer, which is R_{MS} = 23.6 nm. The surface of YBCO layer is rougher than the underlying layers, which can be easily expected.

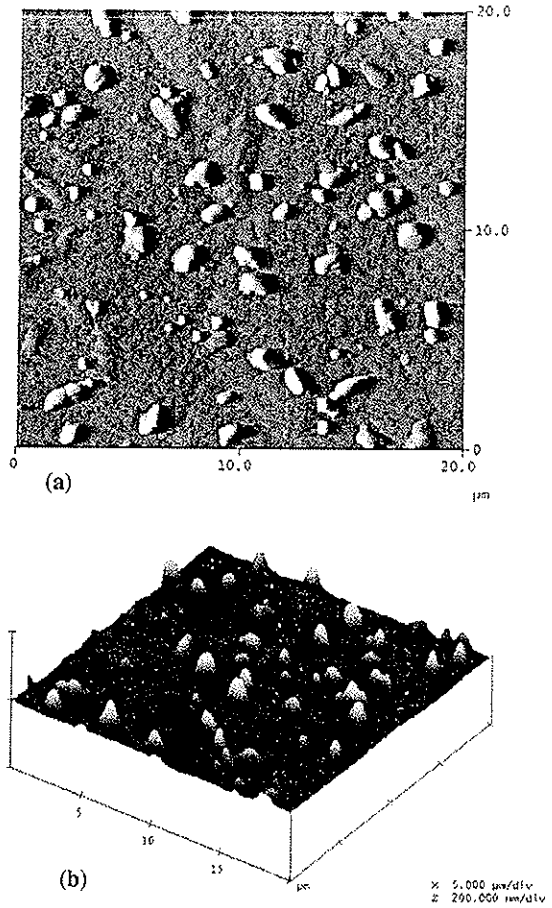

Figure 6. AFM image showing the surface morphology and roughness of the YBCO layer: (a) 2D deflection image; (b) 3D height image.

4. Conclusions

The biaxially textured composite tape of Ni–4.5% Mn/Ni–1.5% Cr was used as the substrate for a coated conductor through the RABiTS approach in order to reduce the ferromagnetism and to increase the mechanical strength. Multi-layer $CeO_2/YSZ/Y_2O_3$ buffer layers were deposited on the substrate by pulsed laser deposition. The Y_2O_3 layer was deposited in two steps at Ar/4% H_2 gas and vacuum in order to obtain a good biaxial texture seed layer and prevent the formation of NiO. The biaxial textures of buffer layers have been obtained on Ni–4.5% Mn/Ni–1.5% Cr substrates. The thickness of the YSZ barrier layer was important to achieve a high J_c of YBCO film, and the threshold thickness was ~300 nm. Cross-sectional SEM and EDS were used to identify the presence of NiO and Ni–Mn–O layers at the buffer–substrate interface. The Ni–Mn–O layer was found to form a uniform layer between Y_2O_3 and Ni–4.5% Mn with thickness of 30 nm, which was supposed to limit further NiO growth to between 5 and 10 nm in thickness. The best J_c of YBCO films deposited by PLD on top of the $CeO_2/YSZ/Y_2O_3$/(Ni–4.5% Mn/Ni–1.5% Cr) was about 1.5×10^6 A cm^{-2} at 77 K and self-field.

Acknowledgments

The samples were prepared and the T_c, I_c measurements together with cross-sectional SEM images were obtained at the Korea Electrotechnology Research Institute, where the research was supported by a grant from the Center for Applied Superconductivity Technology of the 21st Century Frontier R&D Programme (funded by the Ministry of Science and Technology, Republic of Korea). Other measurements were obtained at the Institute for Superconducting and Electronic Materials, University of Wollongong.

References

[1] Kakimoto K, Iijima Y and Saitoh T 2000 *Physica* C **392–396** 783–9
[2] Wu X D, Foltyn S R, Arendt P, Townsend J, Adams C, Campbell I H, Tiwari P, Coulter Y and Peterson D E 1994 *Appl. Phys. Lett.* **65** 1961
[3] Norton D P *et al* 1996 *Science* **274** 755
[4] Goyal A *et al* 1996 *Appl. Phys. Lett.* **69** 1795
[5] Paranthaman M *et al* 2000 *J. Mater. Res.* **15** 2647
[6] List F A, Goyal A, Paranthaman M, Norton D P, Specht E D, Lee D F and Kroeger D M 1998 *Physica* C **302** 87
[7] Goyal A, Paranthaman M P and Schoop U 2004 *MRS Bull.* (August) 552
[8] Finnemore D K, Gray K E, Maley M P, Welch D O, Christen D K and Kroeger D M 1999 *Physica* C **320** 1
[9] Yoshino H, Yamazaki M and Thanh T D 2003 *Physica* C **392–396** 847
[10] Varesi E, Celentano G, Petrisor T, Boffa V, Ciontea L, Galluzzi V, Gambardella U, Mancini A, Rufoloni A and Vannozzi A 2003 *Supercond. Sci. Technol.* **16** 498
[11] Goyal A *et al* 2002 *Physica* C **382** 251
[12] Leonard K J, Goyal A, Kang S, Yarborough K A and Kroeger D M 2004 *Supercond. Sci. Technol.* **17** 1295
[13] Shi D Q, Ko R K, Song K J, Chung J K, Ha H S, Kim H S, Moon S H, Yoo S I and Park C 2005 *Supercond. Sci. Technol.* **18** 561
[14] Ijaduola A O, Thompson J R, Goyal A, Thieme C L H and Marken K 2004 *Physica* C **403** 163
[15] de Boer B, Eickemeyer J, Reger N, Fernandez G-R L, Richter J, Holzapfel B, Schultz L, Prusseit W and Berberich P 2001 *Acta Mater.* **49** 1421